Journal for ImmunoTherapy of Cancer

CLDN18.2 and 4-1BB bispecific antibody givastomig exerts antitumor activity through CLDN18.2-expressing tumor-directed T-cell activation

Jing Gao,[1,2] Zhengyi Wang,[3] Wenqing Jiang,[3] Yanni Zhang,[3] Zhen Meng,[3] Yanling Niu,[3] Zhen Sheng,[3] Chan Chen,[3] Xuejun Liu,[3] Xi Chen,[3] Chanjuan Liu,[3] Keren Jia ,[4] Cheng Zhang,[4] Haiyan Liao,[1] Jaeho Jung,[5] Eunsil Sung,[5] Hyejin Chung,[5] Jingwu Z. Zhang,[6] Andrew X. Zhu,[3] Lin Shen [2,4]

To cite: Gao J, Wang Z, Jiang W, *et al*. CLDN18.2 and 4-1BB bispecific antibody givastomig exerts antitumor activity through CLDN18.2-expressing tumor-directed T-cell activation. *Journal for ImmunoTherapy of Cancer* 2023;**11**:e006704. doi:10.1136/jitc-2023-006704

► Additional supplemental material is published online only. To view, please visit the journal online (http://dx.doi.org/10.1136/jitc-2023-006704).

JG and ZW contributed equally.

Accepted 21 May 2023

For numbered affiliations see end of article.

Correspondence to
Dr Lin Shen;
linshenpku@163.com

Dr Andrew X. Zhu;
andrew.zhu@i-mabbiopharma.com

Dr Jingwu Z. Zhang;
jingwu.zang@i-mabbiopharma.com

ABSTRACT

Background Claudin18.2 (CLDN18.2) is a tight junction protein that has been identified as a clinically proven target in gastric cancer. Stimulation of 4-1BB with agonistic antibodies is also a promising strategy for immunotherapy and 4-1BB$^+$ T cells were reported to be present within the tumor microenvironment of patients with gastric cancer. However, hepatotoxicity-mediated by 4-1BB activation was observed in clinical trials of agonistic anti-4-1BB monoclonal antibodies.

Methods To specifically activate the 4-1BB$^+$ T cells in tumor and avoid the on-target liver toxicity, we developed a novel CLDN18.2×4-1BB bispecific antibody (termed 'givastomig' or 'ABL111'; also known as TJ-CD4B or TJ033721) that was designed to activate 4-1BB signaling in a CLDN18.2 engagement-dependent manner.

Results 4-1BB$^+$ T cells were observed to be coexisted with CLDN18.2$^+$ tumor cells in proximity by multiplex immunohistochemical staining of tumor tissues from patients with gastric cancer (n=60). Givastomig/ABL111 could bind to cell lines expressing various levels of CLDN18.2 with a high affinity and induce 4-1BB activation in vitro only in the context of CLDN18.2 binding. The magnitude of T-cell activation by givastomig/ABL111 treatment was closely correlated with the CLDN18.2 expression level of tumor cells from gastric cancer patient-derived xenograft model. Mechanistically, givastomig/ABL111 treatment could upregulate the expression of a panel of pro-inflammatory and interferon-γ-responsive genes in human peripheral blood mononuclear cells when co-cultured with CLDN18.2$^+$ tumor cells. Furthermore, in humanized 4-1BB transgenic mice inoculated with human CLDN18.2-expressing tumor cells, givastomig/ABL111 induced a localized immune activation in tumor as evident by the increased ratio of CD8$^+$/regulatory T cell, leading to the superior antitumor activity and long-lasting memory response against tumor rechallenge. Givastomig/ABL111 was well tolerated, with no systemic immune response and hepatotoxicity in monkeys.

Conclusions Givastomig/ABL111 is a novel CLDN18.2×4-1BB bispecific antibody which has the potential to treat patients with gastric cancer with a wide range of CLDN18.2 expression level through the restricted activation of 4-1BB$^+$ T cells in tumor microenvironment to avoid the risk of liver toxicity and systemic immune response.

WHAT IS ALREADY KNOWN ON THIS TOPIC

⇒ CD137 (4-1BB), a co-stimulatory receptor, is a uniquely compelling target for cancer immunotherapy. However, hepatotoxicity was observed in clinical trials with agonistic anti-4-1BB monoclonal antibodies due to the activation of 4-1BB signaling on liver myeloid cells.

WHAT THIS STUDY ADDS

⇒ In this study, coexistence and close proximity of claudin18.2 (CLDN18.2)$^+$ tumor cells and 4-1BB$^+$ immune cells were observed in gastric cancer/gastroesophageal junction cancer tissues. Therefore, we developed a novel bispecific antibody, givastomig/ABL111, targeting both CLDN18.2 and 4-1BB to restrict activation of 4-1BB signaling pathway within the tumor microenvironment. A strong and long-lasting antitumor activity was achieved without hepatotoxicity and cytokine release syndrome after treatment with givastomig/ABL111.

HOW THIS STUDY MIGHT AFFECT RESEARCH, PRACTICE OR POLICY

⇒ The results from this study provided strong evidence to support the development of an ongoing phase I clinical trial, which is evaluating the safety, efficacy, pharmacokinetics, and pharmacodynamics of givastomig/ABL111 in patients with advanced solid tumors.

INTRODUCTION

In recent years, immunotherapy has become a transformative therapeutic option for cancer treatment. Various antibodies against different checkpoints, including cytotoxic T lymphocyte-associated protein-4, programmed cell death protein-1 (PD-1), and PD-1 ligand, have been clinically approved

in multiple tumor types. However, the overall objective response rate (ORR) is only approximately 15–30%, and the majority of patients do not respond to immune checkpoint inhibitors.[1 2] Novel therapeutics with tumor-targeted immune activation features acting through multiple co-stimulatory pathways such as CD28, CD137, CD40, are being developed to increase the efficacy of immunotherapies.[3 4]

CD137 (4-1BB, TNFRSF9) is an inducible co-stimulatory molecule that belongs to the tumor necrosis factor (TNF) receptor superfamily. It is expressed on activated T cells that have encountered cognate antigen, activated natural killer (NK) cells, Foxp3$^+$ regulatory T cell (Treg) cells and other immune cells. CD137L/4-1BBL, identified as a unique functional ligand, is expressed on professional antigen-presenting cells such as activated macrophages, B cells, and dendritic cells.[5] The 4-1BB/4-1BBL signaling triggers TNF receptor-associated factors (TRAFs)-mediated activation of NF-κB[5–7] and MAPK signaling pathways,[8] and increased release of cytokines, such as interleukin-2 (IL-2), IL-6, IL-12, TNF, and interferon-γ (IFN-γ).[9] 4-1BB co-stimulates CD8$^+$ T cells through promoting proliferation, differentiation, survival, and cytotoxicity.[10] 4-1BB also enhances NK cell proliferation and IFN-γ production.[11] These studies demonstrate that 4-1BB plays important roles in both innate and adaptive immunity. Urelumab is the first agonistic anti-4-1BB antibody that has been developed in clinical trials, however severe hepatotoxicity was observed in patients treated with urelumab.[12] Utomilumab is another 4-1BB antibody that exhibits milder hepatotoxicity, but the efficacy is suboptimal.[13] Thus, multiple strategies are being explored to activate 4-1BB signaling within the tumor microenvironment (TME) and minimize liver toxicity including intratumoral (IT) administration of 4-1BB antibody, bispecific antibodies that target 4-1BB and a tumor antigen, and 'masked' antibodies that become 'exposed' by tumor-specific protease activity.[14]

The tight junction molecule, claudin18.2 (CLDN18.2), is an attractive tumor-specific antigen for antibody-based immunotherapy. In normal healthy tissue, CLDN18.2 is exclusively expressed in differentiated gastric mucosal membrane epithelial cells.[15 16] However, it is widely expressed in various tumors, including lung cancer,[17] gastric cancer (GC),[16 18] esophageal cancer,[15 19] pancreatic cancer,[20] and colorectal cancer.[21] The biological characteristics of CLDN18.2, including highly restricted expression pattern in normal tissues, frequent ectopic activation in different types of cancers, involvement in tumor development and progression, and location in the outer cell membrane, have paved the way for the development of CLDN18.2-targeted therapies for solid tumor.[15] Zolbetuximab (IMAB362) is the first CLDN18.2-targeted treatment under clinical development. It exerts potent antitumor activity through antibody-dependent cellular cytotoxicity (ADCC), complement-dependent cytotoxicity (CDC), induction of apoptosis, and inhibition of cell proliferation.[19 22] In combination with chemotherapy of epirubicin, oxaliplatin, and capecitabine (EOX), zolbetuximab achieved an ORR of 39.0% versus 25.0% (p=0.034), and a duration of response of 32.6 weeks versus 21.7 weeks (p=0.023) when compared with EOX alone in patients with CLDN18.2-positive advanced gastric cancer (GC) and gastroesophageal junction (GEJ) cancer in the first-line setting.[23] Recent presentation of ongoing phase III SPOTLIGHT/GLOW trials examining zolbetuximab or placebo combined with either FOLFOX or CAPOX-based chemotherapy as first-line treatment for CLDN18.2-positive, HER2-negative advanced GC/GEJ cancer met the primary endpoint of improvement of progression-free survival.[24 25] Owing to the tumor specificity of CLDN18.2, other anti-CLDN18.2 based targeted therapeutics such as antibody-drug conjugates and bispecific T-cell engagers have been developed.[26]

In this study, we observed the presence of 4-1BB$^+$ immune cells in tumor tissues from patients with GC which were surrounded by the CLDN18.2$^+$ tumor cells in a proximity. Therefore, we designed a novel bispecific antibody (BsAb) with one arm that binds to CLDN18.2 and the other arm that targets 4-1BB which enables the clustering and activation of 4-1BB in the context of CLDN18.2 binding, thereby restricting the 4-1BB stimulatory activity within the TME. Our in vitro and in vivo results demonstrated that this BsAb stimulated 4-1BB signaling and subsequent T-cell activity in a CLDN18.2-dependent manner. In a mouse model, this BsAb elicited a strong and long-lasting antitumor activity with localized immune activation, without induction of systemic immune response and hepatic toxicity. Collectively, our data indicate that CLDN18.2-targeted 4-1BB activation is a potential therapeutic for the treatment of solid tumors, with limited adverse effects.

MATERIALS AND METHODS

Multiplex immunohistochemistry

Three panels of five-plex fluorescent immunohistochemistry (IHC) assay were conducted on formalin-fixed and paraffin-embedded (FFPE) tumor tissues from 60 patients with GC. Panel 1: CLDN18.2 (ab222512; 1:500; Abcam), CD4 (ZM0418; 1:500; ZSBIO), 4-1BB (CST34594; 1:300; Cell Signaling Technology), Foxp3 (BLG320202; 1:300; BioLegend), and PanCK (CST4545; 1:800; Cell Signaling Technology). Panel 2: CLDN18.2 (ab222512; 1:500; Abcam), CD8A (CST70306; 1:500; Cell Signaling Technology), PD-1 (CST86163; 1:100; Cell Signaling technology), 4-1BB (CST34594; 1:300; Cell Signaling Technology), and PanCK (CST4545; 1:800; Cell Signaling Technology). Panel 3: CD8A (CST70306; 1:500; Cell Signaling Technology), CD47 (CST63000; 1:400; Cell Signaling Technology), CD68 (CST76437; 1:500; Cell Signaling Technology), CD163 (CST93498; 1:500; Cell Signaling Technology) and PanCK (CST4545; 1:800; Cell Signaling Technology). Images were acquired using the Mantra Quantitative Pathology Imaging System (PerkinElmer). The multispectral images were visualized

in a Phenochart. Image analysis on counting of cells, with either uniquely stained or concurrently stained markers within regions of interest (ROI) was performed on scanned images. The representative ROIs were chosen by two specialist pathologists. To quantify the spatial distribution of tumor-infiltrating immune cells and tumor cells, an effective score was established. Within a radius of 20 or 30 µm, the central CLDN18.2$^+$ tumor cells and the surrounding 4-1BB$^+$CD4$^+$ or 4-1BB$^+$CD8$^+$ T cells were paired. Effective score was calculated by dividing the number of 4-1BB$^+$CD4$^+$ or 4-1BB$^+$CD8$^+$ T cells paired with CLDN18.2$^+$ tumor cells by the total number of CLDN18.2$^+$ tumor cells.[27]

Surface plasmon resonance

Surface plasmon resonance (SPR) experiments were performed on a Biacore T200 instrument (GE HealthCare). The filtered HBS-EP buffer (HEPES 10 mM, NaCl 150 mM, EDTA 3 mM, 0.005% Tween 20, pH7.4) was used as the running buffer. To analyze the binding kinetics between human CLDN18.2 and antibodies, a CLDN18.2 virus-like particle (VLP, Kactus) was captured on the surface of the CM5 chip. Serial 1.5-fold diluted antibodies (givastomig/ABL111: ranging from 666.7 nM to 131.7 nM; zolbetuximab: ranging from 1820 nM to 359.5 nM) were injected over the chip surface at a flow rate of 30 µL/min. The association phase was monitored for 60 s and the dissociation phase was monitored for 1200 s. To measure the binding kinetics between givastomig/ABL111 and 4-1BB, givastomig/ABL111 was captured on flow cell 2 with human Fc antibody domain. Serial twofold diluted 4-1BB protein (ranging from 100 nM to 6.25 nM) were injected for 90 s at a flow rate of 30 µL/min. At the end of the sample injection, the buffer was injected for 300 s to monitor the dissociation.

ELISA binding assays

The 96-well plate (Thermo Scientific) was coated with 3 µg/mL of CLDN18.1 or CLDN18.2 VLPs (Kactus) and incubated at 4°C overnight. Then the plate was washed and blocked with 3% bovine serum albumin at 37°C for 1 hour. The threefold or fivefold serial dilutions of test antibodies with a starting concentration of 100 nM were added into the pre-coated plate and then incubated at 37°C for 1 hour. Next, the plate was washed and incubated with mouse anti-human IgG Fc secondary antibody (GenScript Biotech) at 37°C for 1 hour. The substrate (CoWin Biotech) and stop solutions (0.5 mol/L H_2SO_4) were added and OD450 was acquired by the EnVision plate reader (PerkinElmer).

Cell-based binding assays by flow cytometry

Flow cytometry was used to analyze the binding ability of the test molecules to CLDN18.2-positive cancer cell lines, including CHO-K1 expressing human CLDN18.2 cells and SNU620 cells (Genomeditech). The serial threefold dilutions of givastomig/ABL111, the reference antibody zolbetuximab, and human IgG were prepared in MACS buffer (phosphate buffered saline (PBS), 2% fetal bovine serum, 2 mM EDTA). Final concentration was starting from 100 nM. The diluted antibodies were added into the cell suspension at a density of 1×10^5 cells/well and incubated for 30 min on ice. Subsequently, the cells were washed with a MACS buffer once to remove unbound antibodies, followed by incubation with Alexa Fluor 633-conjugated anti-human IgG (H+L) secondary antibody (Invitrogen) at 4°C for 30 min. Lastly, the cells were washed with a MACS buffer to remove unbound secondary antibody. Fluorescence measurement was acquired on FACSCelesta Flow Cytometer (BD Biosciences) and analyzed in FlowJo to determine the mean fluorescence intensities.

Reporter cell line assays

The activation of 4-1BB pathway was investigated using a luciferase reporter assay. The NF-κB reporter Jurkat cell line overexpressing human 4-1BB (NF-κB/4-1BB reporter Jurkat cell line, Promega) was co-cultured with the CHO-K1 cells overexpressing human CLDN18.2 (CLDN18.2$^+$) or parental CHO-K1 cells (CLDN18.2$^-$) (Genomeditech). Serially diluted antibodies were incubated with the cell co-cultures at a final concentration starting from 20 µg/mL at 37°C for 6 hours. Luminescence was obtained by adding the Bio-Glo Reagent (Promega, G7940) and measured by the plate reader (BMG LABTECH).

T-cell activation assays

The in vitro T-cell activation mediated by testing antibodies was characterized by co-culturing anti-CD3 pre-activated human peripheral blood mononuclear cells (PBMCs) and target cells, including the CLDN18.2$^+$ CHO-K1 cell line and cells isolated from four gastric adenocarcinoma patient-derived xenograft (PDX) models expressing CLDN18.2 at different levels (GA0006, GA0044, GA0060 and GA3055, Crownbio HuPrime animal facility). The microplate was coated with anti-CD3 antibody at a final concentration of 0.5 µg/mL at 4°C overnight, or 37°C for 1 hour. Human PBMCs were seeded at a density of 1×10^5 cells/well into the pre-coated plates. The target cells (2.5×10^4 cells/well) were incubated with the pre-activated PBMCs, with effector to target (E:T) cell ratio of 4:1. Antibodies were serially diluted and added to the cell co-cultures at a final concentration starting from 20 nM or 10 nM. After 48 hours of incubation at 37°C, level of IL-2 in the supernatant was measured by homogeneous time-resolved fluorescence resonance energy transfer (PerkinElmer).

NanoString analysis

Human PBMCs (three donors, 0.5×10^6 cells/well) were co-cultured with the CHO-K1-hCLDN18.2 cells (0.125×10^6) with E:T ratio of 4:1 in the presence of 0.5 µg/mL anti-CD3 (555336, BD Biosciences) and 20 nM givastomig/ABL111 or isotype control hIgG. The cell co-cultures were incubated at 37°C for 24 hours. PBMCs were

then collected for RNA extraction. About 100 ng RNA were extracted from each sample for NanoString analysis using NanoString nCounter PanCancer Human Immune Profiling Panel. After positive control linearity check and background correction, the passed gene counts in all samples from nCounter platform were normalized by median of ratio method based on house-keeping genes which were selected by geNorm algorithm.[28] Differential expression test was performed on the normalized gene count data using the paired Student's t-test. The genes with absolute fold change larger than 1.5 and p value less than 0.05 were selected as statistically differentially expressed genes, which were used for downstream immune cell type and functional analysis.

In vivo tumor efficacy model

Female C57BL/6-*Tnfrsf9*$^{tm1(TNFRSF9)}$ (humanized h4-1BB, Beijing Biocytogen) mice at the age of 6–8 weeks were subcutaneously inoculated with human CLDN18.2 expressing MC38 (MC38$^{hCLDN18.2}$) colon carcinoma tumor cells (5×10^5 cells/mouse). The animals were treated biweekly with the following six regimens: hIgG (3 mg/kg), CLDN18.2 monoclonal antibody (mAb) (the same clone as givastomig/ABL111, 3 mg/kg), 4-1BB mAb (the same clone as givastomig/ABL111, 3 mg/kg), CLDN18.2 mAb (3 mg/kg) plus 4-1BB mAb (3 mg/kg), givastomig/ABL111 (4 mg/kg), and zolbetuximab (3 mg/kg). The tumor volumes were monitored twice a week. At day 54 after primary tumor injection, the givastomig/ABL111-cured mice were rechallenged with another subcutaneous injection of MC38$^{hCLDN18.2}$ cells. The tumor volumes were monitored up to 38 days after tumor rechallenge. Previously untreated sex and age-matched mice (naïve) were used as the control mice for tumor rechallenge. For each treatment regimen, a satellite group treated with three doses of antibodies was used for evaluation of tumor-infiltrating lymphocytes (TILs) by fluorescence-activated cell sorting (FACS).

To study whether givastomig/ABL111 has a dose-dependent antitumor efficacy, h4-1BB mice inoculated with the MC38$^{hCLDN18.2}$ cell line were treated with hIgG and givastomig/ABL111 (0.4, 1, 2, 5, or 10 mg/kg) every week for three cycles. The satellite groups treated with one dose of antibodies were used for evaluation of TILs by FACS. In addition, the expression of Foxp3, 4-1BB, NKp46, PD-1, and CD8 in tumors from hIgG-treated mice and 5 mg/kg givastomig/ABL111-treated mice was analyzed by multiplex IHC.

Toxicity study in cynomolgus monkeys

For toxicology evaluation, a total of 40 cynomolgus monkeys (*Macaca fascicularis*) were randomly assigned to four groups with five animals/sex/group and intravenously administered givastomig/ABL111 one time per weekly for five doses (0, 10, 30 or 100 mg/kg/dose). All groups consisted of three animals/sex/group for a terminal sacrifice at Day 30, and two animals/sex/group undergoing an additional 6-week treatment-free period for evaluation of potential reversibility, persistence or delayed effect. The animals were monitored for mortality, clinical signs, local irritation, body weights, food consumption, and ophthalmic examinations. Safety pharmacology assessment included body temperatures, ECG, blood pressure, heart rate, respiration, and neurological examinations. Laboratory investigations included clinical pathology (hematology, coagulation, serum chemistry, and urinalysis), immunology (anti-drug antibody analysis, immunophenotyping, cytokine analysis), and toxicokinetics. At study termination, a full list of tissues was taken from all animals for organ weight recording, gross necropsy observation and microscopic examinations.

In vitro cytokine release assay

An in vitro cytokine release assay was conducted by co-culturing human PBMCs and CHO-K1-hCLDN18.2 cells. Phytohemagglutinin (PHA), anti-CD3 and anti-CD3/CD28 served as the positive controls, and isotype control and PBS as the negative controls. Givastomig/ABL111 at 0.015, 0.15 and 1.5 µM were tested in this in vitro system. Following a 24-hour incubation at 37°C, the cell culture supernatant was collected and cytokines including TNF-α, IFN-γ, IL-1β, IL-2, IL-4, IL-6, IL-8, IL-10, IL-12, p70, and granulocyte-macrophage colony-stimulating factor (GM-CSF) were measured using MSD kits (K151A0H-1 and K151A0H-2, Meso Scale Discovery).

RESULTS

Infiltration of 4-1BB-positive immune cells in CLDN18.2-positive tumors of patients with GC/GEJ cancer

To investigate the tumor-infiltrating immune cell profiles of patients with GC, we used multiplex immunohistochemistry (mIHC) to stain for different characteristic markers of immune cells and tumor cells of FFPE tumor specimens from 60 Chinese patients with GC/GEJ cancer. The baseline characteristics of these patients with GC/GEJ cancer were presented in table 1 and the mIHC panels were depicted in figure 1A. Forty-five out of 60 patients (75%) had CLDN18.2-positive tumors which was defined as ≥40% tumor cells with ≥1+ staining intensity (figure 1B). Next, we analyzed the density of various tumor-infiltrating immune cell subsets in the CLDN18.2-positive tumor tissues from patients with GC/GEJ cancer and found a higher infiltration of CD4$^+$ T cells, CD8$^+$ T cells, total macrophages (CD68$^+$) and M2 macrophages (CD68$^+$CD163$^+$) accompanied with less infiltration of Treg cells (CD4$^+$Foxp3$^+$) (figure 1C). More important, we found the presence of total 4-1BB$^+$ immune cells, 4-1BB$^+$CD4$^+$ T cells, and 4-1BB$^+$CD8$^+$ T cells in CLDN18.2$^+$ tumor tissues (figure 1D). We further investigated the spatial organization of 4-1BB$^+$CD4$^+$ T cells and 4-1BB$^+$CD8$^+$ T cells near tumor cells in the CLDN18.2$^+$ GC/GEJ cancer tissues. Within a radius of 20 or 30 µm, the central CLDN18.2$^+$ tumor cells and the surrounding 4-1BB$^+$CD4$^+$ or 4-1BB$^+$CD8$^+$ T cells were paired. The representative images are shown in figure 1E. To quantify both cell

Table 1 Patient characteristics

Characteristics	All (n=60)	CLDN18.2$^+$ group (n=45)	CLDN18.2$^-$ group (n=15p)	p value
Age				
Median	59.5 (22–74)	61 (24–74)	58 (22–74)	
Gender				
Male	48 (80%)	37 (82%)	11 (73%)	0.709
Female	12 (20%)	8 (18%)	4 (27%)	
ECOG PS				
0	36 (60%)	29 (64%)	7 (47%)	0.224
1	24 (40%)	16 (36%)	8 (53%)	
Location				
GEJ	14 (23%)	10 (22%)	4 (27%)	1.000
Non-GEJ	46 (77%)	35 (78%)	11 (73%)	
Lauren classification				
Intestinal type	26 (43%)	21 (47%)	5 (33%)	0.556
Diffuse type	17 (28%)	11 (24%)	6 (40%)	
Mixed type	17 (28%)	13 (29%)	4 (27%)	
Differentiation				
Moderate	16 (27%)	14 (31%)	2 (13%)	0.227
Moderate–poor	18 (30%)	11 (24%)	7 (47%)	
Poor	26 (43%)	20 (44%)	6 (40%)	
4-1BB level				
≥Median 4-1BB density	30 (50%)	22 (49%)	8 (53%)	0.766
<Median 4-1BB density	30 (50%)	23 (51%)	7 (47%)	

CLDN18.2, claudin18.2; ECOG PS, eastern cooperative oncology group performance status; GEJ, gastroesophageal junction.

proximity and quantity of CD4$^+$4-1BB$^+$ and CD8$^+$4-1BB$^+$ T cells in the tumor region, the effective score was defined as the number of CD4$^+$4-1BB$^+$ or CD8$^+$4-1BB$^+$ T cells within a radius of 20 or 30 µm distance to CLDN18.2$^+$ tumor cells divided by the total number of CLDN18.2$^+$ tumor cells. Across the two distances (0–20 µm and 0–30 µm) evaluated, both CD4$^+$4-1BB$^+$ T cells and CD8$^+$4-1BB$^+$ T cells were present. A higher effective score was observed in a 30 µm distance than that in a 20 µm distance, indicating a higher density of 4-1BB$^+$ T cells around the CLDN18.2$^+$ tumor cells within a broader spatial area (figure 1F).

Generation of CLDN18.2-targeting 4-1BB BsAb

The existence of 4-1BB$^+$ immune cells nearby CLDN18.2$^+$ tumor cells in patients with GC promoted us to design a BsAb targeting both CLDN18.2 and 4-1BB. The CLDN18.2×4-1BB BsAb, givastomig/ABL111 was constructed by fusing a single-chain variable fragment targeting h4-1BB to the C terminus of the anti-hCLDN18.2 IgG1 antibody, with a single amino acid substitution (N300A) on the Fc region (figure 2A). Givastomig/ABL111 was designed to simultaneously bind both CLDN18.2$^+$ tumor cells and 4-1BB$^+$ T cells to induce the 4-1BB activation signal in the context of CLDN18.2 engagement (figure 2B). As measured by SPR, givastomig/ABL111 bound to CLDN18.2 VLP with a high affinity (K_D=1.698×10^{-10} M, figure 2C). The binding selectivity of givastomig/ABL111 was also confirmed that it could bind to CLDN18.2 with an EC_{50} of 0.13 nM (figure 2D) but not to CLDN18.1 (online supplemental figure S1A). We also characterized the binding of givastomig/ABL111 to cell surface CLDN18.2 where cell lines expressing different levels of CLDN18.2 were used. As shown in figure 2E, givastomig/ABL111 showed a stronger binding affinity to all the tested cells expressing high, medium and even low level of CLDN18.2 than the control monoclonal antibody. Since givastomig/ABL111 was designed to eliminate Fc-effector function via a single amino acid substitution (N300A) on the Fc region, we further evaluated ADCC and CDC of the BsAb. The results confirmed that givastomig/ABL111 did not induce any ADCC and CDC effects against CLDN18.2-expressing or 4-1BB-expressing cells, whereas anti-4-1BB or anti-CLDN18.2 antibody with wildtype IgG1 elicited significant ADCC and CDC activity (online supplemental figure S1B–D).

Givastomig/ABL111 induces 4-1BB agonism in a CLDN18.2 engagement-dependent manner

In addition to the CLDN18.2 arm, we investigated the 4-1BB arm of this BsAb. First, the binding affinity of givastomig/ABL111 against human 4-1BB protein was measured by SPR with a K_D of 9.88×10^{-9} M (figure 3A). Second, by using a luciferase NF-κB/4-1BB reporter Jurkat cell line, givastomig/ABL111 induced stronger intensity of 4-1BB activation than 4-1BB monoclonal antibody urelumab when co-cultured with CLDN18.2$^+$ cell lines. However, without CLDN18.2 engagement, givastomig/ABL111 did not activate the 4-1BB pathway whereas urelumab still induced strong 4-1BB signaling (figure 3B). Consistent with the results of 4-1BB signaling, givastomig/ABL111 exhibited a significantly higher production of IL-2 in anti-CD3 pre-activated PBMCs than urelumab in the presence of CHO-K1 cells expressing CLDN18.2 while there was no induction of IL-2 by givastomig/ABL111 treatment in the presence of control CHO-K1 cells (figure 3C). Moreover, we evaluated the activation of T cells by givastomig/ABL111 treatment when co-cultured with tumor cells from GC PDXs expressing different levels of CLDN18.2. The IHC staining and expression level of CLDN18.2 for each PDX sample was depicted in figure 3D. The data showed that givastomig/ABL111 stimulated IL-2 production in a dose-dependent manner and the increased level was closely correlated with that of CLDN18.2 expression on tumor (figure 3E). These data collectively indicated that givastomig/ABL111 exerted 4-1BB stimulation and subsequent T-cell activation only in the context of CLDN18.2 engagement.

Givastomig/ABL111 shifts towards a pro-inflammatory gene expression profile in activated PBMCs

To delineate the activation-related features induced by givastomig/ABL111, we co-cultured human PBMCs pre-activated

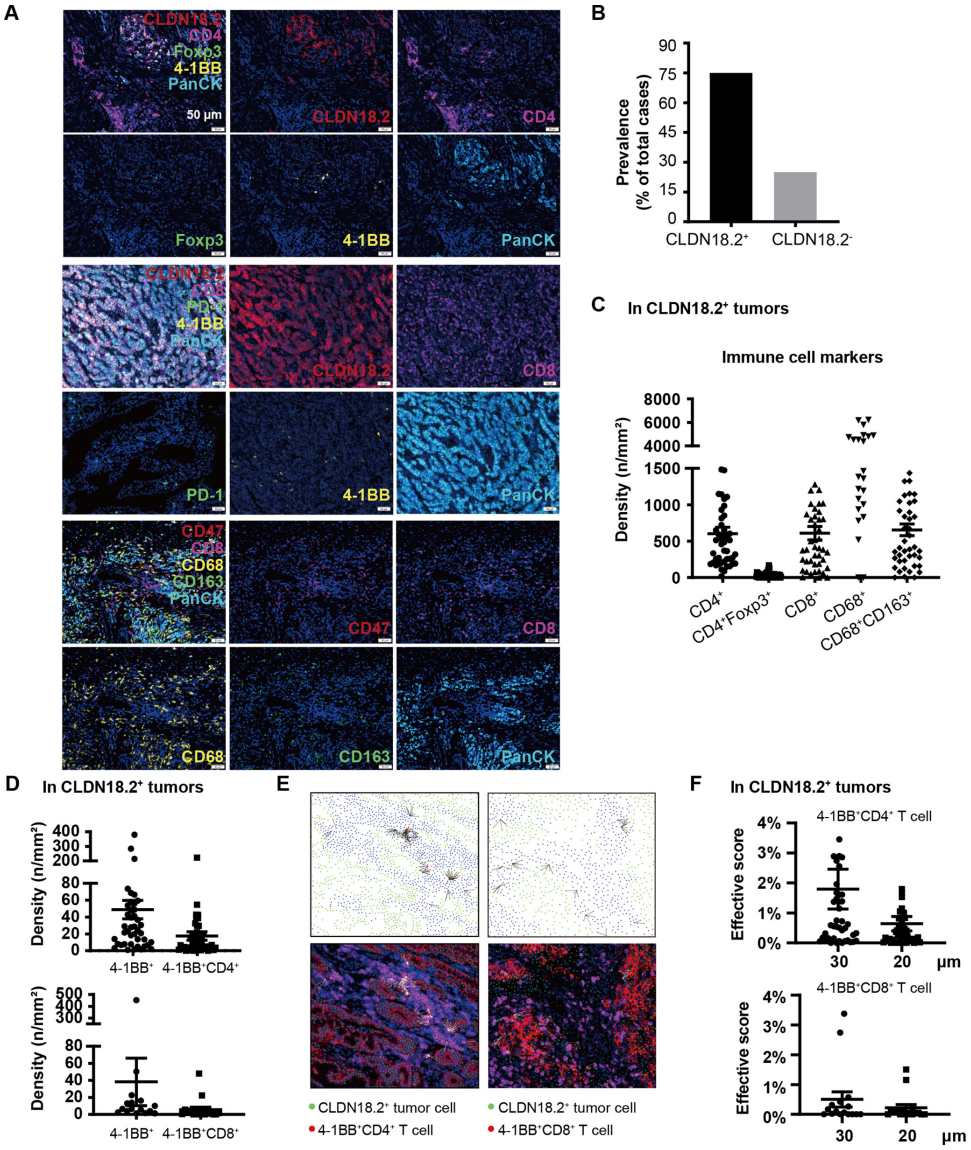

Figure 1 Characterization of the tumor microenvironment in CLDN18.2-positive tumors from patients with GC/GEJ cancer. (A) The representative images for three panels of five-plex multiplex immunohistochemistry. Panel 1 (upper) included CLDN18.2, CD4 (helper T cell), Foxp3 (regulatory T cell), 4-1BB, and PanCK (tumor marker). Panel 2 (middle) included CLDN18.2, CD8 (cytotoxic T cell), PD-1, 4-1BB, and PanCK (tumor marker). Panel 3 (lower) included CD47, CD8 (cytotoxic T cell), CD68 (pan macrophage), CD163 (M2 macrophage), and PanCK (tumor marker). (B) The prevalence of cases with CLDN18.2-positive and CLDN18.2-negative tumors. Tissues with any specific staining intensity in ≥40% of tumor cells were defined as CLDN18.2 positivity. (C) The density of immune cell types in CLDN18.2-positive GC/GEJ cancer tissues. (D) The density of 4-1BB$^+$ immune cells, including total 4-1BB$^+$ cells, 4-1BB$^+$CD4$^+$ T cells, and 4-1BB$^+$CD8$^+$ T cells, in CLDN18.2-positive GC/GEJ cancer tissues. (E) Illustration of the spatial analysis involving CLDN18.2$^+$ tumor cells and 4-1BB$^+$ T cells. The green dot represents the CLDN18.2$^+$ tumor cell and the red dot represents 4-1BB$^+$CD4$^+$ or 4-1BB$^+$CD8$^+$ T cell. The black line connects a red dot and a green dot within 30 μm distance. (F) The effective score is obtained by dividing the number of 4-1BB$^+$CD4$^+$ or 4-1BB$^+$CD8$^+$ T cells around CLDN18.2$^+$ tumor cells within 20 μm or 30 μm radius by the total number of CLDN18.2$^+$ tumor cells. Data are presented as mean±SEM. CLDN18.2, claudin18.2; GC, gastric cancer; GEJ, gastroesophageal junction; PD-1, programmed cell death protein-1.

with anti-CD3 antibody to induce 4-1BB expression with human CLDN18.2 CHO-K1 cell lines in the presence of givastomig/ABL111 and performed a NanoString analysis of differential gene expression in collected PBMCs using PanCancer Immune Profiling Panel. The results showed that givastomig/ABL111 treatment upregulated a set of pro-inflammatory gene expression including IL-2, IFN-γ, TNF, CSF2, TNFRSF9, etc and downregulated a set of anti-inflammatory gene expression including PDCD1, ARG2, TGFB2, etc (figure 4A). Pathway analysis showed that the expression of gene signatures reflecting inflammation, NF-κB pathway, NK cell activation, and T-cell activation were increased by givastomig/ABL111 treatment, whereas the expression of genes representing T cell/NK cell co-inhibitory checkpoint, regulator of T cell and TGFβ pathway was decreased (figure 4B). Hence, the NanoString analysis

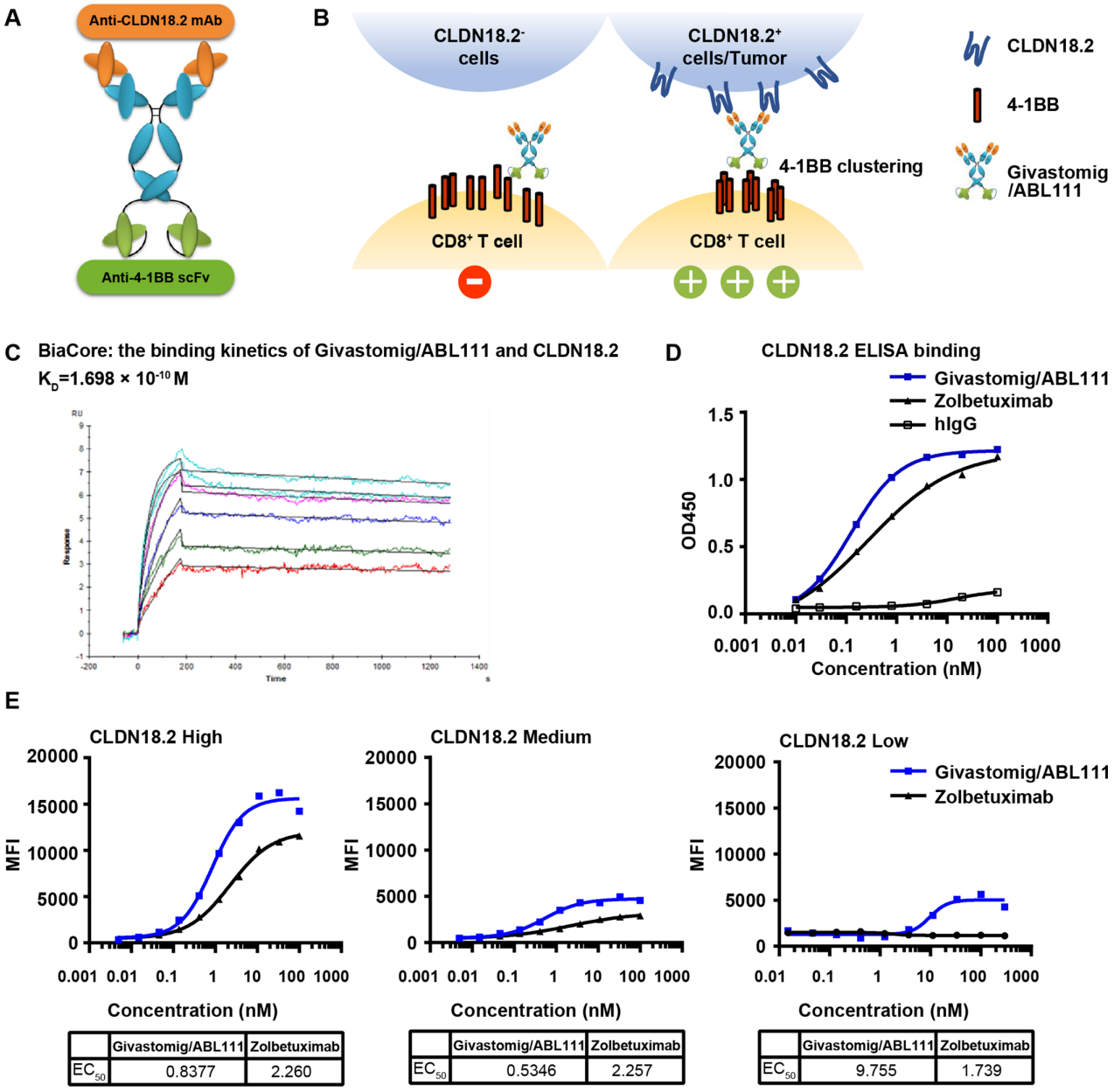

Figure 2 Development of human CLDN18.2-dependent 4-1BB agonistic bispecific antibody (givastomig/ABL111). (A) Givastomig/ABL111 was designed to target both CLDN18.2 and 4-1BB. N300A mutation was introduced to prevent the Fc portion from binding FcγR. (B) Illustration showing the mechanism of action of givastomig/ABL111. (C) The Biacore analysis was performed to measure the binding affinity between givastomig/ABL111 and CLDN18.2 VLP. (D) ELISA assay showing the binding of serial concentrations of givastomig/ABL111 and zolbetuximab to CLDN18.2 VLP. (E) CHO-K1 cells overexpressing different levels of human CLDN18.2 and SNU620 cells were incubated with serial concentrations of givastomig/ABL111 and zolbetuximab antibodies. mAb, monoclonal antibody; CLDN18.2, claudin18.2; MFI, mean fluorescence intensities; scFv, single-chain variable fragment; VLP, virus-like particle.

data revealed that givastomig/ABL111 induced the gene expression in anti-CD3 pre-activated PBMCs towards a pro-inflammatory profile to support the underlined mechanism of T-cell activation.

Givastomig/ABL111 exhibits antitumor activity in vivo in humanized mice

We further evaluated the antitumor activity of givastomig/ABL111 in vivo using human 4-1BB transgenic mice subcutaneously engrafted with syngeneic MC38 tumor cells ectopically expressing human CLDN18.2 ($MC38^{hCLDN18.2}$). On day 7 post tumor inoculation, the tumor-bearing mice were treated with zolbetuximab, anti-CLDN18.2 mAb, anti-4-1BB mAb, combination of anti-CLDN18.2 plus anti-4-1BB, or givastomig/ABL111. Compared with the monotherapy with anti-CLDN18.2 or zolbetuximab which did not attenuate tumor progression and monotherapy with anti-4-1BB or combination treatment of anti-4-1BB with anti-CLDN18.2 which induced

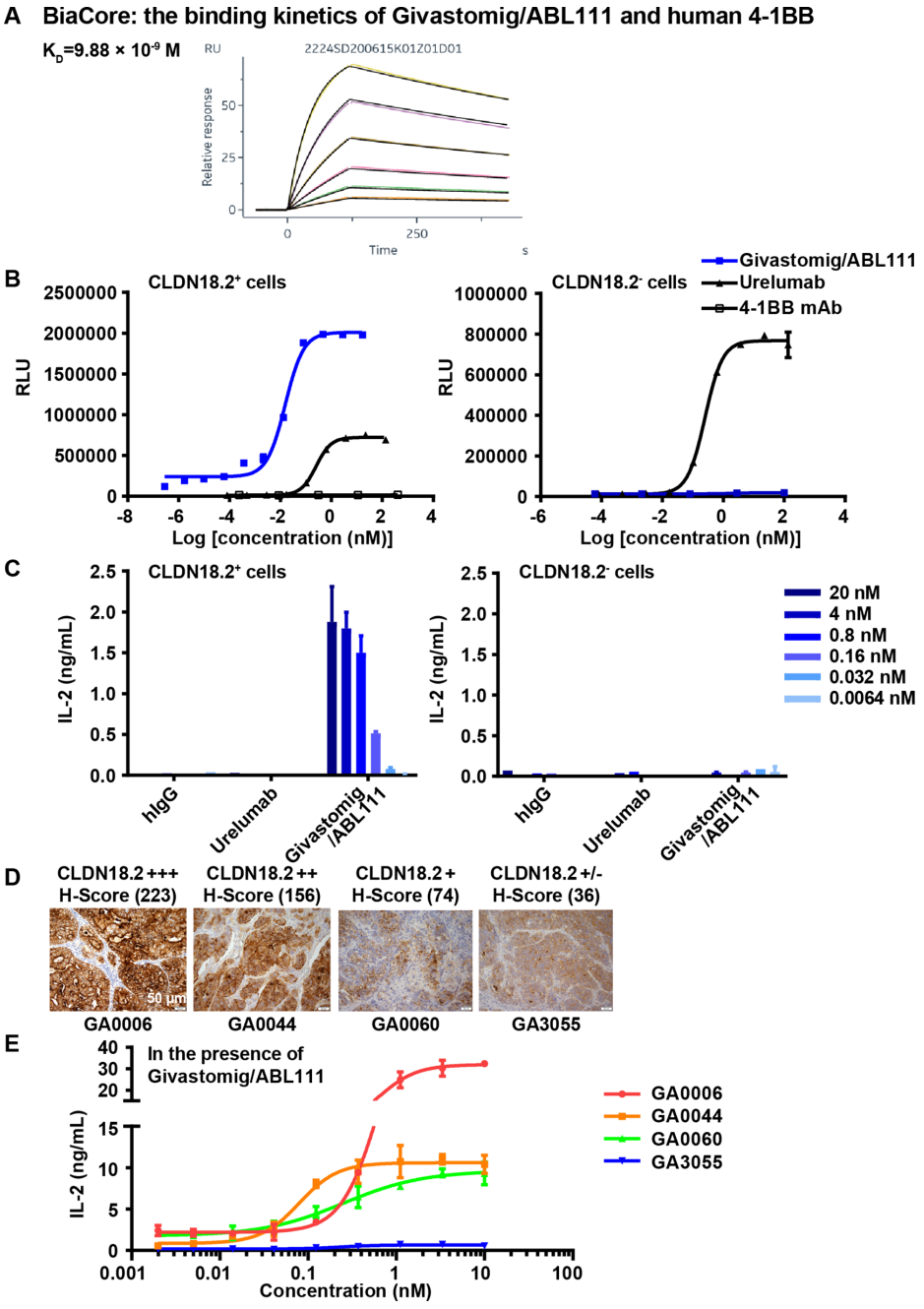

Figure 3 Givastomig/ABL111 activates the NF-κB pathway and T cells in a CLDN18.2 engagement-dependent manner. (A) The binding affinity between givastomig/ABL111 and human 4-1BB protein was evaluated by the Biacore analysis. (B) The NF-κB/4-1BB reporter Jurkat cell line was co-cultured with CHO-K1 cells overexpressing human CLDN18.2 (CLDN18.2$^+$) or parental CHO-K1 cells (CLDN18.2$^-$) in the presence of serial concentrations of givastomig/ABL111, anti-4-1BB mAb and urelumab. Luminescence was obtained by adding the substrate of luciferase and measured by a microplate reader. (C) Anti-CD3 pre-activated human PBMCs were co-cultured with the CLDN18.2$^+$ and CLDN18.2$^-$ CHO-K1 cells in the presence of givastomig/ABL111 and urelumab. IL-2 was measured by homogeneous time-resolved fluorescence resonance energy transfer. (D) Immunohistochemistry staining of CLDN18.2 expression in four gastric cancer PDX samples, coded GA0006, GA0044, GA0060 and GA3055, respectively. Histoscore (H-score) was calculated by a semi-quantitative assessment. (E) Anti-CD3 pre-activated human PBMCs were co-cultured with the target cells from the above four PDXs in the presence of serial concentrations of givastomig/ABL111. The supernatant was collected and the levels of IL-2 were measured. RLU, relative light units; mAb, monoclonal antibody; CLDN18.2, claudin18.2; IL, interleukin; PBMCs, peripheral blood mononuclear cells; PDX, patient-derived xenograft.

partial inhibition of tumor growth, givastomig/ABL111 treatment resulted in almost complete tumor regression with six out of seven mice achieving tumor-free survival (figure 5A). To investigate whether givastomig/ABL111 can generate a long-lasting antitumor immunity, mice that rejected the implanted MC38$^{hCLDN18.2}$ tumor by the

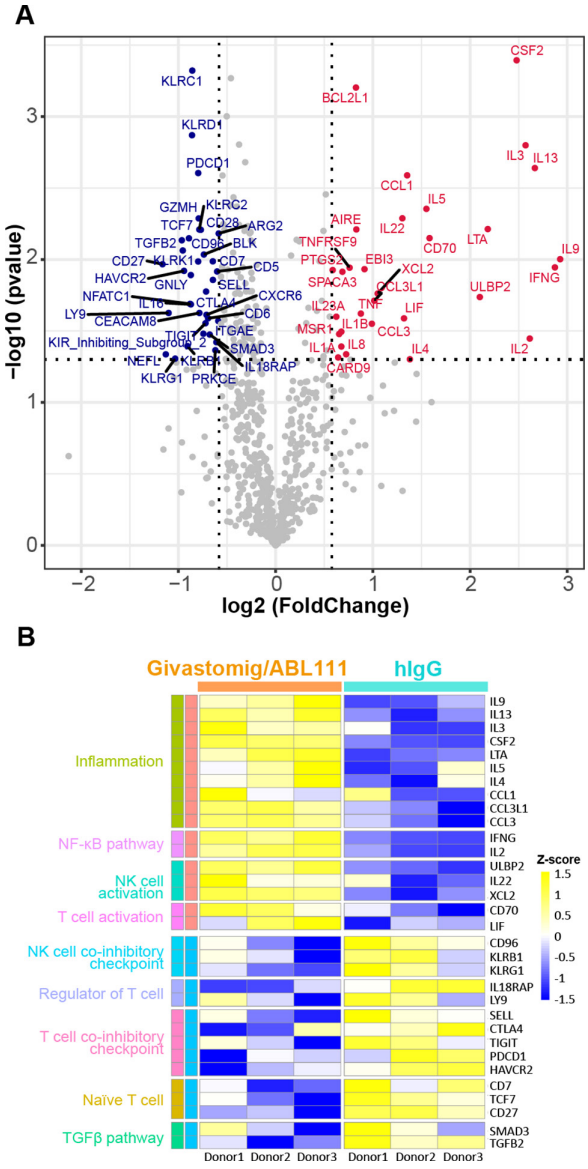

Figure 4 Givastomig/ABL111 induces a pro-inflammatory gene expression profile in PBMCs co-cultured with CLDN18.2-expressing cells. (A) Volcano plot showing statistical significance and fold changes of differential expression of 770 genes in PBMCs between two comparing conditions. The x-axis shows the mean of log2-transformed fold changes in gene expression level in the givastomig/ABL111-treated versus hIgG-treated group. The y-axis shows the log10-transformed p value of paired t-test in expression levels between the two groups. The genes with >1.5-fold upregulation in the givastomig/ABL111-treated group at a significance level of 0.05 are highlighted in red, while those with >1.5-fold downregulation are highlighted in blue. (B) Pathway-annotated expression heatmap of genes significantly modulated by givastomig/ABL111 (fold change >1.5 and p value<0.05). The gene expression values are normalized as Z-score across six samples (columns). IL, interleukin; NK, natural killer; PBMCs, peripheral blood mononuclear cells.

treatment with BsAb were rechallenged 54 days later with a new injection of MC38$^{hCLDN18.2}$ cells. All the givastomig/ABL111-cured mice, but not age-matched naïve mice, were resistant to a rechallenge with MC38$^{hCLDN18.2}$ tumor cells, showing that the BsAb can induce long-term protective immunological memory against tumor (figure 5B). Immunophenotyping analysis of tumors and peripheral blood from tumor bearing mice with different treatments showed that only givastomig/ABL111 induced an increase in CD45$^+$ leukocytes, CD8$^+$ T cells and CD8$^+$/Treg ratio as well as decrease in Treg cells in tumor as compared with other treatment groups (figure 5C). In the peripheral blood, there were no significant changes in these T-cell populations of tested mice among all the treatment groups (online supplemental figure S2A).

To examine the dose-response of givastomig/ABL111 treatment in vivo, we administered different doses of BsAb in the human 4-1BB transgenic mice established with MC38$^{hCLDN18.2}$ tumor cells. Treatment of givastomig/ABL111 exerted a dose-dependent antitumor activity, with a dose of 0.4 mg/kg or 1 mg/kg yielding partial therapeutic efficacy, while a dose of 5 mg/kg or 10 mg/kg achieved complete tumor regression (figure 5D). Consistently, we found a correspondent increase of CD45$^+$ leukocytes and CD8$^+$ T cells in the tumor in a similar dose-dependent manner as confirmed by flow cytometry (figure 5E). Furthermore, we analyzed different cell subsets of tumor infiltrating lymphocytes in tumor resected from IgG control or givastomig/ABL111 (5 mg/kg) treated mice by mIHC staining (online supplemental figure S3A). As compared with IgG control, givastomig/ABL111 treatment induced an increase of IT CD8$^+$ T cells and decrease of total Foxp3$^+$ Tregs and 4-1BB$^+$Foxp3$^+$ Tregs, leading to a significant shift in the CD8$^+$/Treg ratio (online supplemental figure S3B). Therefore, these results indicate that givastomig/ABL111 induced significant antitumor activity in vivo which was superior to anti-CLDN18.2 or anti-4-1BB monotherapy or in combination, accompanied by the increased CD8$^+$ T-cell infiltration in tumor without systemic immune response.

Givastomig/ABL111 is well tolerated in cynomolgus monkeys and does not induce hepatotoxicity and overall immune activation

Finally, we assessed the safety of givastomig/ABL111 in cynomolgus monkeys. We first examined whether givastomig/ABL111 could cross-react with monkey CLDN18.2 and 4-1BB by FACS and Biacore. The results showed that givastomig/ABL111 bound to monkey CLDN18.2 and 4-1BB in comparable affinity with human proteins (online supplemental figure S4A,B). Givastomig/ABL111 treatment was well tolerated by cynomolgus monkeys up to 100 mg/kg, the no-observed-adverse-effect-level defined in the 4-week good laboratory practice (GLP) toxicity study. Liver toxicity has always been encountered for 4-1BB agonist antibody treatment with severe hepatotoxicity as evidenced by elevated transaminases, neutropenia, thrombocytopenia and fatigue. Our data showed that no treatment-related microscopic changes occurred in the liver up to 100 mg/kg (figure 6A). Additionally, no significant changes in the serum level of liver enzyme

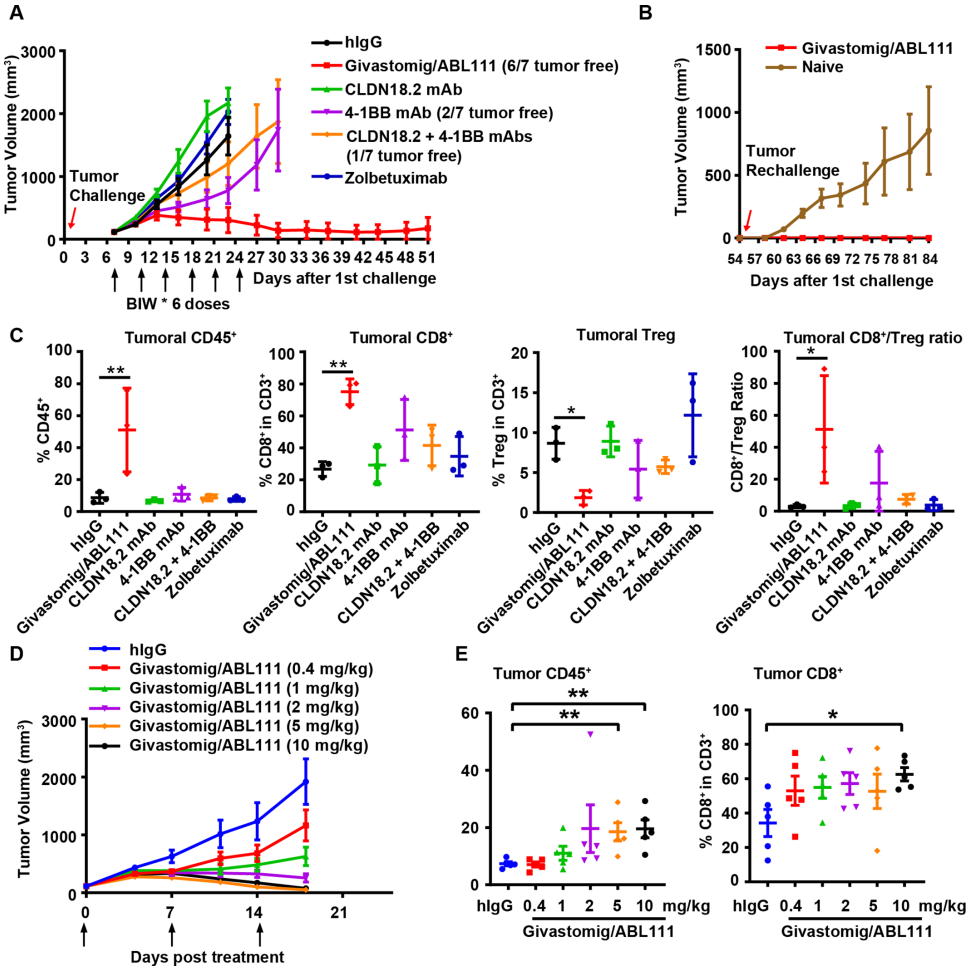

Figure 5 Givastomig/ABL111 treatment exerts antitumor effects in vivo and regulates the immune cell infiltration within the tumor tissues. (A) The humanized transgenic mice expressing human 4-1BB were subcutaneously inoculated with the MC38 cell line expressing human CLDN18.2 (MC38$^{hCLDN18.2}$). The mice were treated biweekly in six different groups and the tumor volumes were monitored twice a week. (B) At 54 days after primary tumor injection, the givastomig/ABL111-cured mice and naïve mice were rechallenged using the same tumor cells. Tumor volumes were presented as mean±SEM. (C) Tumor-infiltrating leukocytes were evaluated by the flow cytometry. The graphs denote the proportion of CD45$^+$ cells, the proportion of CD8$^+$ T cells in CD3$^+$ cells, the proportion of Foxp3$^+$ cells in CD3$^+$ cells, and the CD8$^+$/Treg ratio. (D) The MC38$^{hCLDN18.2}$ mice were treated with serial concentrations of givastomig/ABL111. (E) Tumor-infiltrating CD45$^+$ and CD8$^+$ cells were evaluated by the flow cytometry. Statistical comparison performed with the unpaired t-test. Data are presented as mean±SEM. *p<0.05, **p<0.01. mA, monoclonal antibody; BIW, biweekly; CLDN18.2, claudin18.2; Treg, regulatory T cell.

activities (aspartate aminotransferase and alanine aminotransferase) were observed in each monkey treated with different doses of givastomig/ABL111 as compared with those treated with vehicle control (tables 2 and 3). The highest dose of 100 mg/kg is 1000 times higher than the maximum tolerated dose of urelumab in human (0.1 mg/kg),[29] indicating givastomig/ABL111 administration did not impair normal liver functions or cause structural alterations.

To examine the potential effects of givastomig/ABL111 on the induction of systemic immune activation, overall lymphocytes and subpopulations were monitored in the peripheral blood from all the doses of treated animals and there were no changes noted. Consistently, the results of the in vitro cytokine release assay where the potential of givastomig/ABL111 to activate immune response was evaluated in human PBMCs with CHO-K1 cells expressing CLDN18.2, also confirmed givastomig/ABL111 treatment at different concentrations did not increase the production of various inflammatory cytokines tested, such as GM-CSF, TNF-α, IL-10, IL-6, IL-2, IFN-γ and IL-1β (figure 6B). Collectively, these results demonstrated that givastomig/ABL111 did not elicit systemic immune activation under physiological conditions.

DISCUSSION

Among T-cell co-stimulatory receptors, 4-1BB possesses a unique capability for both activation and pro-inflammatory polarization of tumor-reactive T cells, rendering it a promising target for immunotherapy. While urelumab, the leading agonistic anti-4-1BB mAb, had demonstrated potent antitumor effects in preclinical studies, hepatotoxicity hampered its clinical development.[30] Therefore,

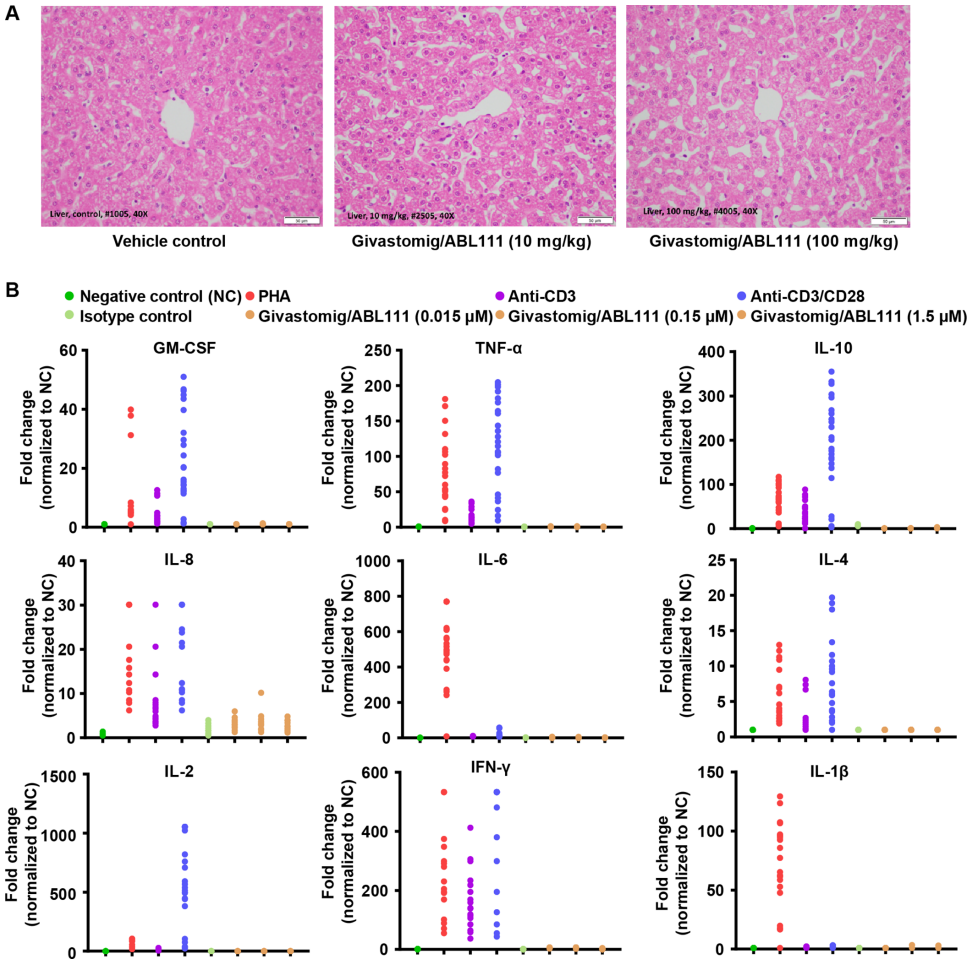

Figure 6 Treatment with givastomig/ABL111 is well tolerated in cynomolgus monkeys. (A) The liver sections in the 4-week monkey toxicity study were stained with H&E and examined microscopically. (B) Human peripheral blood mononuclear cells were co-cultured with or without the CHO-K1-hCLDN18.2 cells at an E:T ratio of 10:1 in the presence of the test molecules. The cell supernatant was collected and the levels of several cytokines was measured by the Meso Scale Discovery method. E:T, effector to target; NC, negative control; GM-CSF, granulocyte-macrophage colony-stimulating factor; PHA, phytohemagglutinin; IFN, interferon; IL, interleukin; TNF, tumor necrosis factor.

restricting 4-1BB activation to the TME by targeting 4-1BB with BsAb that simultaneously engages a tumor associated antigen (TAA) appears to be an attractive approach to reduce hepatotoxicity and systemic immune activation.

Our mIHC analysis of tumor biopsies from patients with GC/GEJ cancer revealed a higher prevalence (75%) for CLDN18.2 positive (defined as ≥40% of tumor staining with ≥1+ staining intensity). In addition, coexistence and close proximity of CLDN18.2$^+$ tumor cells with both 4-1BB$^+$CD4$^+$ and 4-1BB$^+$CD8$^+$ T cells observed in CLDN18.2-positive tumor tissues. Taken together, our data suggests that CLDN18.2 might be a promising TAA for BsAb design in GC/GEJ cancer. Therefore, we developed a novel BsAb, givastomig/ABL111, targeting both CLDN18.2 and 4-1BB to restrict the activation of 4-1BB signaling pathway in a CLDN18.2 engagement-dependent manner.

As reviewed by Wajant,[31] full activation of 4-1BB receptor and downstream signaling by its natural ligand or agonistic antibodies requires not only the initial formation of the receptor-ligand/antibody complex,

Table 2 The alanine aminotransferase levels in cynomolgus monkeys

	hIgG (n=10)		Givastomig/ABL111 (10 mg/kg) (n=10)		Givastomig/ABL111 (30 mg/kg) (n=10)		Givastomig/ABL111 (100 mg/kg) (n=10)		
Study day	Range	Mean±SD	Range	Mean±SD	Range	Mean±SD	Range	Mean±SD	p value
Baseline	14–84	53.3±19.0	51–89	67.5±11.5	40–89	60.6±16.7	33–86	58.4±15.6	0.2691
8	16–68	51.9±14.9	31–69	54.2±11.8	36–82	57.8±16.0	39–143	67.2±29.6	0.318
15	14–53	40.9±12.0	32–71	46.7±13.3	27–64	44.6±10.3	31–82	48.5±13.9	0.5653
29	12–67	41.4±14.8	26–62	47.3±13.1	27–62	49.6±10.2	26–68	48.9±11.1	0.4519

Table 3 The aspartate aminotransferase levels in cynomolgus monkeys

	hIgG (n=10)		Givastomig/ABL111 (10 mg/kg) (n=10)		Givastomig/ABL111 (30 mg/kg) (n=10)		Givastomig/ABL111 (100 mg/kg) (n=10)		
Study day	Range	Mean±SD	Range	Mean±SD	Range	Mean±SD	Range	Mean±SD	p value
Baseline	37–90	54.7±15.1	42–229	82.8±64.3	43–160	73.2±36.4	47–166	80.3±40.6	0.461
8	52–94	65.9±15.3	38–94	65.2±15.9	32–115	82.1±30.2	45–232	102.2±54.4	0.055
15	47–160	68.4±33.7	51–137	89.1±32.6	46–120	72.2±22.8	48–146	95.0±36.6	0.1988
29	38–74	53.7±10.3	51–148	86.1±35.1	40–135	77.1±29.3	50–177	86.8±38.6	0.0677

but also the clustering of such complexes on the plasma membrane of T cells. Clustering of receptor-antibody complex on T cells can be mediated by binding of Fcγ receptors to the Fc domain of the agonistic antibodies, such as utomilumab or AGEN2373.[32 33] In our study, givastomig/ABL111 is engineered to eliminate the Fc-effector function via a single amino acid substitution (N300A) on the Fc domain, and thereby the Fcγ receptors mediated clustering of 4-1BB-givastomig/ABL111 complexes. Instead, the structural hallmark of givastomig/ABL111 is that it induces the clustering of 4-1BB complex on T cells only on binding to CLDN18.2. This feature is mainly caused by the unique binding epitope of the 4-1BB arm of givastomig/ABL111 which is located in the proximal CRD4 domain resulting in the optimal spacing of 4-1BB clustering and subsequent T-cell activation.

Compared with anti-CLDN18.2 mAb zolbetuximab, givastomig/ABL111 exhibited higher binding affinity to CLDN18.2-expressing cells at different levels of CLDN18.2. In particular, givastomig/ABL111 bound to the cell line with low CLDN18.2 expression while zolbetuximab did not. In the co-culture system of anti-CD3 stimulated PBMCs and GC cells from four PDXs, givastomig/ABL111 induced IL-2 release when the target cells were isolated from the PDX with low CLDN18.2 expression. These data suggests that givastomig/ABL111 might elicit 4-1BB activation in TME in patients with low CLDN18.2 expression.

As expected, the anti-4-1BB mAb urelumab induced the activation of 4-1BB and downstream NF-κB signaling in T cells regardless of the presence of nearby CLDN18.2-expressing cells. By contrast, activation of 4-1BB signaling in T cells by givastomig/ABL111 was highly dependent on its engagement with CLDN18.2 on nearby target cells. These results demonstrated that 4-1BB activation by givastomig/ABL111 was restricted to the TME and systematic T-cell activation was minimized.

Keren *et al* reported that CLDN18.2-positive tumors were identified in more than 50% of patients with GC and the CLDN18.2-positive group showed significantly higher total $CD8^+$ T cells and $CD4^+$ T cells.[27] Additionally, transcriptional analysis in the previous study revealed that GC was classified as 'IFN-γ dominant' immune subtype, which was associated with high infiltration of $CD8^+$ T cells.[34] Because of the high prevalence of CLDN18.2 expression, the high infiltration of immune cells, and coexistence of $CLDN18.2^+$ tumor cells and $4\text{-}1BB^+$ immune cells in GC, givastomig/ABL111 could be positioned as a potential novel therapy for patients with GC. In addition, CLDN18.2 is highly expressed in multiple cancers, especially in those of the digestive system, including GC, GEJ cancer, esophageal cancer, pancreatic cancer, etc, and givastomig/ABL111 might also be a potential targeted therapy in these cancer types. Chemotherapy and immunotherapies have already been used in combination with the 4-1BB mAbs urelumab or utomilumab to explore synergistic or additive antitumor effects. Several classes of chemotherapies showed synergistic effects in combination with the 4-1BB antibody in preclinical studies, by enhancing the proliferation of $CD8^+$ cells or inducing 4-1BB expression,[35–38] suggesting that the combination therapy of givastomig/ABL111 and chemotherapy may present a useful treatment strategy.

Givastomig/ABL111 displayed similar binding affinities to both CLDN18.2 and 4-1BB in humans and monkeys. Therefore, the toxicological profiles characterized in cynomolgus monkeys have translational relevance to humans. In the 4-week GLP toxicity study, givastomig/ABL111 was well tolerated by cynomolgus monkeys. No hepatotoxicity was observed throughout the study period. Systemic immune activation was also absent as evidenced by lack of peripheral immune cell increase (data not shown) or cytokine elevation.

In summary, our study presents a novel anti-4-1BB×CLDN18.2 BsAb (givastomig/ABL111). Its specific design ensures that 4-1BB co-stimulation mediated by this molecule is in a CLDN18.2 engagement-dependent manner. Givastomig/ABL111 treatment induced a strong antitumor effect in multiple animal models, and there were no systemic immune response and hepatic toxicity in GLP toxicity study. Our study provides the strong rationale for clinical development of this agent and a phase I study of givastomig/ABL111 in advanced solid tumors is ongoing to examine its safety, efficacy, pharmacokinetics, and pharmacodynamics (NCT04900818).

Author affiliations
[1]Department of Oncology, Shenzhen Key Laboratory of Gastrointestinal Cancer Translational Research, Cancer Institute, Peking University Shenzhen Hospital,

Shenzhen-Peking University-Hong Kong University of Science and Technology Medical Center, Shenzhen, China
[2]SIP LifeLink Oncology Research Institute, Suzhou, China
[3]I-Mab Biopharma, Shanghai, China
[4]Department of Gastrointestinal Oncology, Peking University Cancer Hospital and Institute, Beijing, China
[5]ABL Bio Inc, Seongnam, Republic of Korea
[6]I-Mab Biopharma, Gaithersburg, Maryland, USA

Acknowledgements We express our sincere appreciation to the National Natural Science Foundation of China (No. 82072728)) for the grants. We thank the authors from I-Mab Biopharma for antibody development. We also thank authors and Mr Jaehyoung Jeon and Mr Youngkwang Kim from ABL Bio for antibody development.

Contributors Conception and design: JG, ZW, JZZ, AXZ, and LS. Antibody development: ZW, WJ, YZ, ZM, JJ, ES, HC, JZZ, and AXZ. In vitro study: JG, ZW, WJ, YZ, ZM, CC, XC, and CL. Animal experiment: JG, ZW, WJ, YZ, ZM, and CC. Analysis and interpretation of data: all authors. Writing of the manuscript: ZW, YN, and LS. Study supervision: JZZ, AXZ, and LS. LS is responsible for the overall content as guarantor.

Funding This work was supported by the National Natural Science Foundation of China (No. 82072728).

Competing interests ZW, WJ, YZ, ZM, YN, ZS, CC, XL, XC, CL, JZZ, and AXZ are employees of I-Mab Biopharma and JJ, ES, and HC are employees of ABL Bio which develop antibodies presented in this manuscript.

Patient consent for publication Not applicable.

Ethics approval This study involves human participants, is a retrospective study and the formalin-fixed and paraffin-embedded samples of patients were used for multiplex immunohistochemistry analysis. This study is exempted by ethics committee(s) or institutional board(s). Informed consent was obtained from all individual participants. We have updated this part in the manuscript.

Provenance and peer review Not commissioned; externally peer reviewed.

Data availability statement Data are available upon reasonable request.

ORCID iDs
Keren Jia http://orcid.org/0000-0001-6577-0573
Lin Shen http://orcid.org/0000-0002-8798-4756

REFERENCES

1 Seidel JA, Otsuka A, Kabashima K. Anti-PD-1 and anti-CTLA-4 therapies in cancer: mechanisms of action, efficacy, and limitations. *Front Oncol* 2018;8:86.
2 Zhao B, Zhao H, Zhao J. Efficacy of PD-1/PD-L1 blockade monotherapy in clinical trials. *Ther Adv Med Oncol* 2020;12.
3 Mayes PA, Hance KW, Hoos A. The promise and challenges of immune agonist antibody development in cancer. *Nat Rev Drug Discov* 2018;17:509–27.
4 Choi Y, Shi Y, Haymaker CL, *et al*. T-cell agonists in cancer Immunotherapy. *J Immunother Cancer* 2020;8.
5 Croft M. The role of TNF Superfamily members in T-cell function and diseases. *Nat Rev Immunol* 2009;9:271–85.
6 Jang IK, Lee ZH, Kim YJ, *et al*. Human 4-1Bb (Cd137) signals are mediated by Traf2 and activate nuclear factor-Kappa B. *Biochem Biophys Res Commun* 1998;242:613–20.
7 Arch RH, Thompson CB. 4-1Bb and Ox40 are members of a tumor necrosis factor (TNF)-Nerve growth factor receptor Subfamily that bind TNF receptor-associated factors and activate nuclear factor kappaB. *Mol Cell Biol* 1998;18:558–65.
8 Cannons JL, Choi Y, Watts TH. Role of TNF receptor-associated factor 2 and P38 mitogen-activated protein kinase activation during 4-1Bb-dependent immune response. *J Immunol* 2000;165:6193–204.
9 Hashimoto K. Cd137 as an attractive T cell Co-stimulatory target in the TNFRSF for Immuno-oncology drug development. *Cancers (Basel)* 2021;13.
10 Wen T, Bukczynski J, Watts TH. 4-1Bb ligand-mediated Costimulation of human T cells induces Cd4 and Cd8 T cell expansion, cytokine production, and the development of Cytolytic Effector function. *J Immunol* 2002;168:4897–906.
11 Makkouk A, Chester C, Kohrt HE. Rationale for anti-Cd137 cancer Immunotherapy. *Eur J Cancer* 2016;54:112–9.
12 Segal NH, Logan TF, Hodi FS, *et al*. Results from an integrated safety analysis of Urelumab, an agonist anti-Cd137 Monoclonal antibody. *Clin Cancer Res* 2017;23:1929–36.
13 Segal NH, He AR, Doi T, *et al*. Phase I study of single-agent Utomilumab (PF-05082566), a 4-1Bb/Cd137 agonist, in patients with advanced cancer. *Clin Cancer Res* 2018;24:1816–23.
14 Chester C, Sanmamed MF, Wang J, *et al*. Immunotherapy targeting 4-1Bb: mechanistic rationale, clinical results, and future strategies. *Blood* 2018;131:49–57.
15 Sahin U, Koslowski M, Dhaene K, *et al*. Claudin-18 splice variant 2 is a pan-cancer target suitable for therapeutic antibody development. *Clin Cancer Res* 2008;14:7624–34.
16 Singh P, Toom S, Huang Y. Anti-Claudin 18.2 antibody as new targeted therapy for advanced gastric cancer. *J Hematol Oncol* 2017;10:105.
17 Micke P, Mattsson JSM, Edlund K, *et al*. Aberrantly activated Claudin 6 and 18.2 as potential therapy targets in non-small-cell lung cancer. *Int J Cancer* 2014;135:2206–14.
18 Hashimoto I, Oshima T. Claudins and gastric cancer: an overview. *Cancers (Basel)* 2022;14.
19 Sahin U, Schuler M, Richly H, *et al*. A phase I dose-escalation study of Imab362 (Zolbetuximab) in patients with advanced gastric and Gastro-Oesophageal junction cancer. *Eur J Cancer* 2018;100:17–26.
20 Wöll S, Schlitter AM, Dhaene K, *et al*. Claudin 18.2 is a target for Imab362 antibody in Pancreatic Neoplasms. *Int J Cancer* 2014;134:731–9.
21 Iwaya M, Hayashi H, Nakajima T, *et al*. Colitis-associated colorectal adenocarcinomas frequently Express Claudin 18 Isoform 2: implications for Claudin 18.2 Monoclonal antibody therapy. *Histopathology* 2021;79:227–37.
22 Türeci Özlem, Mitnacht-Kraus R, Wöll S, *et al*. Characterization of Zolbetuximab in Pancreatic cancer models. *Oncoimmunology* 2019;8.
23 Sahin U, Türeci Ö, Manikhas G, *et al*. FAST: a randomised phase II study of Zolbetuximab (Imab362) plus EOX versus EOX alone for first-line treatment of advanced Cldn18.2-positive gastric and Gastro-Oesophageal adenocarcinoma. *Ann Oncol* 2021;32:609–19.
24 Shitara K, Lordick F, Bang Y-J, *et al*. Zolbetuximab plus Mfolfox6 in patients with Cldn18.2-positive, Her2-negative, untreated, locally advanced Unresectable or metastatic gastric or Gastro-Oesophageal junction adenocarcinoma (SPOTLIGHT): a Multicentre, randomised, double-blind, phase 3 trial. *Lancet* 2023;401:1655–68.
25 Xu R, Shitara K, Ajani JA, *et al*. Zolbetuximab + CAPOX in 1L Claudin-18.2+ (Cldn18.2+)/Her2− locally advanced (LA) or metastatic gastric or gastroesophageal junction (mG/GEJ) adenocarcinoma: primary phase 3 results from GLOW. *JCO* 2023;41.(36_suppl)
26 Cao W, Xing H, Li Y, *et al*. Claudin18.2 is a novel molecular biomarker for tumor-targeted Immunotherapy. *Biomark Res* 2022;10:38.
27 Jia K, Chen Y, Sun Y, *et al*. Multiplex immunohistochemistry defines the tumor immune Microenvironment and Immunotherapeutic outcome in Cldn18.2-positive gastric cancer. *BMC Med* 2022;20:223.
28 Vandesompele J, De Preter K, Pattyn F, *et al*. Accurate normalization of real-time quantitative RT-PCR data by Geometric averaging of multiple internal control genes. *Genome Biol* 2002;3.
29 Timmerman J, Herbaux C, Ribrag V, *et al*. Urelumab alone or in combination with Rituximab in patients with Relapsed or refractory B-cell lymphoma. *Am J Hematol* 2020;95:510–20.
30 Chester C, Ambulkar S, Kohrt HE. 4-1Bb Agonism: adding the accelerator to cancer Immunotherapy. *Cancer Immunol Immunother* 2016;65:1243–8.
31 Wajant H. Principles of antibody-mediated TNF receptor activation. *Cell Death Differ* 2015;22:1727–41.

32 Fisher TS, Kamperschroer C, Oliphant T, *et al*. Targeting of 4-1Bb by Monoclonal antibody PF-05082566 enhances T-cell function and promotes anti-tumor activity. *Cancer Immunol Immunother* 2012;61:1721–33.
33 Galand C, Venkatraman V, Marques M, *et al*. 377 Agen2373 is a Cd137 agonist antibody designed to leverage optimal Cd137 and FcγR Co-targeting to promote antitumor immunologic effects. 35th Anniversary Annual Meeting (SITC 2020); 2020:A229–30
34 Thorsson V, Gibbs DL, Brown SD, *et al*. The immune landscape of cancer. *Immunity* 2018;48:812–30.
35 Kim YH, Choi BK, Kim KH, *et al*. Combination therapy with cisplatin and Anti-4-1Bb: synergistic anticancer effects and Amelioration of cisplatin-induced nephrotoxicity. *Cancer Res* 2008;68:7264–9.
36 Kim K-M, Kim HW, Kim J-O, *et al*. Induction of 4-1Bb (Cd137) expression by DNA damaging agents in human T lymphocytes. *Immunology* 2002;107:472–9.
37 Kim YH, Choi BK, Oh HS, *et al*. Mechanisms involved in synergistic anticancer effects of Anti-4-1Bb and cyclophosphamide therapy. *Mol Cancer Ther* 2009;8:469–78.
38 Park JY, Jang MJ, Chung YH, *et al*. Doxorubicin enhances Cd4(+) T-cell immune responses by inducing expression of Cd40 ligand and 4-1Bb. *Int Immunopharmacol* 2009;9:1530–9.